

Validation of Fast Site-Specific Mean-Value Models for Indoor Propagation

¹C. W. Trueman, ¹D. Davis, ²B. Segal, and ³W. Muneer

¹ Department of Electrical and Computer Engineering, Concordia University, Montreal, Canada
trueman@ece.concordia.ca , don@ece.concordia.ca

² McGill University and SMBD Jewish General Hospital, Montreal, Canada
b_segal@sympatico.ca

³ Department of Electrical and Computer Engineering, University of British Columbia, Vancouver, Canada
wadahmuneer@yahoo.co.uk

Abstract – A fast assessment of the local mean value of the electric field strength throughout a floor plan is useful for the design of local-area networks. Site-specific models require coding the location of walls, doorways, and other features and modelling their structure and electrical properties. Using ray tracing to find the field strength throughout the floor plan is slow and expensive because a grid of closely-spaced points is needed to trace the rapid variations called fast fading; then the *ray-tracing local area average* is found by explicit spatial averaging, to obtain the slow fading behavior. The *ray-tracing mean value* is obtained by combining the amplitudes of the fields associated with the rays on an energy basis; widely-spaced grid points can be used because the local mean value varies slowly with position, making the calculation fast and inexpensive. The *Sabine method* provides a energy-balance approach for an inexpensive estimate of the local mean value field strength. This paper tests the accuracy of the fast methods (the ray-tracing mean value and the Sabine mean value) against the local area average found from dense ray tracing, and against measurements. In a 40 m² room of roughly square floor plan, the fields from the fast methods were close to those of dense ray tracing and to the measurements. But it is shown that in a long corridor, the ray-tracing mean value and the Sabine mean value were low compared to dense ray tracing, and so these fast methods should be used with caution.

I. INTRODUCTION

Indoor propagation is the study of the electric field strength due a transmitter operating at a given location and frequency in the floor plan of a building [1, 2]. A “site-specific model” uses the actual location of the walls, windows, doors, and other major features of a floor plan in a three-dimensional model. The location of a transmitter is specified, and a model of the behavior of

the field is used to predict the electric field strength throughout the floor plan. If there are many transmitters, such as the access points of a wireless local area network, it is necessary to assess the coverage of each individual transmitter. Also, if two or more transmitters operate on the same frequency, the signal-to-interference ratio at each point in the floor plan is needed. To assess electromagnetic interference with other equipment, the location of mobile transmitters must be known, and the net field strength due to all transmitters must be estimated. For problems with many sources, a fast, inexpensive estimate of the field strength over the whole floor plan due to each individual source is required.

A recent paper [3] uses the array decomposition fast multiple method to obtain a full-wave solution for the fields in a classroom at 2.4 GHz. The technique offers accuracy that may be better than ray tracing, and permits furniture to be included in the model, such as an array of chairs. A finite-difference method based on transmission-line modelling and the “multiresolution frequency domain parflow method” is used in [4] to solve the system of equations. The fields of a 2.4 GHz transmitter are found in a floor plan having eight rooms and a hallway, using a two-dimensional (2D) approximation. The finite-difference time-domain method is used in [5] to solve a 2D model of a floor plan having several rooms and hallways, at 900 MHz. The internal details of walls, such as pipes and ducts, can be represented in this approach. The authors comment that a slab wall model is not a good representation of a wall constructed of blocks having internal hollow spaces. However, 2D approximations do not account for the floor or ceiling and hence cannot predict the variation of the field with height above the floor. None of these models can be considered inexpensive or “fast” for computation.

The “log distance path loss model” [1, 2, 6, 7, 8] represents the local mean power as declining with distance in an indoor environment according to P_0 / r^n ,

where P_0 is the power at 1 m distance, and n is the “path loss exponent” [8] or “slope index” [6]. This model is empirical in nature with the value of n determined from measured received powers [7]. When the ray joining the source to the receiver passes through a wall, a wall attenuation factor is used to account for the transmission loss. The attenuation can be dependent on the type of wall, and is often derived from measurements. This model makes minimal use of the site-specific nature of the model, and relies on values of n determined by measurement from similar sites, rather than deduced from the construction and electrical properties of the walls. This model is very fast for computation but has limited accuracy.

Ray tracing (RT) is commonly used to analyze site-specific models [8-10]. The transmitter and observer are joined by a straight-line path called the “direct” ray. The field strength is that of the transmitter in free space, attenuated by transmission through walls in the path of the ray. The transmitter and receiver are joined by many reflected rays, including single reflections from the walls, the floor or the ceiling, double reflections involving two room surfaces, multiple reflections, and indeed transmission through one or more walls. The net field strength due to all the reflected rays together is the “multipath field” [3]. Attenuation due to reflection or transmission is often accounted for by modelling walls as uniform layered structures, sometimes called “slab walls,” and using polarization- and angle-dependent reflection and transmission coefficients [11]. Diffraction from edges can also be accounted for [2]. Ray tracing is considered to provide good accuracy for site-specific field calculation. As the number of reflections that is accounted for increases, the cost of the ray-tracing computation increases sharply. If ray tracing is used to identify N ray paths joining a transmitter (Tx) to a receiver (Rx) and each ray path has an associated complex-valued vector electric field, \bar{E}_k for $k = 1, \dots, N$, the local electric field vector at the observer is given by the “vector sum method” [12] as,

$$\bar{E} = \sum_{k=1}^N \bar{E}_k. \quad (1)$$

The magnitude of the electric field strength is assessed by combining the vector components on an energy basis.

A. Slow Fading, Fast Fading and the Ray-Tracing Local Area Average

As the observer moves, the length of each ray path changes, with an associated phase change, leading to the rapid fluctuation in the local electric field strength with distance called “fast fading” [1, 2]. These rapid variations are often removed by spatial averaging to find the

underlying “slow fading”. The resulting average value is variously called the “local mean power” [13], the “sector average” [6], the “local mean signal strength” [12], or the “local area average” [2]. A local-area-average field strength can be calculated by averaging the local field strength on a power basis over an area S according to,

$$\tilde{E} = \sqrt{\frac{1}{S} \iint E^2 ds} \quad (2)$$

but this is rarely done due to the computational cost of evaluating the electric field over a grid of closely-spaced points. The area average is often approximated with a linear average,

$$\tilde{E}_{LAA} = \sqrt{\frac{1}{\Delta} \int E^2 d\ell} \quad (3)$$

where ℓ is distance along the path and Δ is the averaging interval, called the *window size* in this paper, and is typically 5 to 40 wavelengths [2, 6]. Windowing smoothes out the rapid fluctuations associated with fast fading, and reveals the slow fading associated with the attenuation of the field strength with distance travelled, and due to shadowing by the walls and other obstructions in the floor plan. In [1, 2, 9, 14, 15], the field strength is measured around a circular path and the integral around the circumference is used to approximate the local area average of the field strength at the center of the circle. The average value of the signal along a straight-line path with a window size of “twenty or so” wavelengths is termed the “sector average” in [6].

Using ray tracing to compute the field strength over a grid of points spaced by approximately a tenth of the wavelength is sufficient to predict the fast fading of the electric field strength. Then an explicit spatial average can be evaluated over an area with equation (2), or along a straight-line path with equation (3), to find the local mean field strength. In this paper, the *ray-tracing local area average* (RTLAA) is obtained using equation (3) with a path length of about six wavelengths.

B. Ray-Tracing Mean Value

The phase of the field associated with each ray arriving at an observer is often assumed to be a random variable with a uniform distribution [1]. Then the field strength at the observer is also a random variable, with a Rayleigh distribution if there is no dominant component, or a Rician distribution if one component, such as the direct field, is much larger than other components [1]. Then an estimate of the mean value of the random variable is obtained at a single point by the “power sum method” [12, 16] by combining the field strengths of the individual rays \bar{E}_k for $k = 1, \dots, N$ on an energy basis according to,

$$\tilde{E}_{MV} = \sqrt{\sum_{k=1}^N |E_k|^2} \quad (4)$$

which in this paper equation (4) will be called the *ray-tracing mean value* (RTMV) field strength. The sum in equation (4) is proportional to the volume-averaged energy density in the field, and is expected to vary slowly with position, because the ray amplitudes vary slowly with position, whereas the phases vary rapidly.

The computation of the RTLAA is expensive because a dense grid of points is needed to trace fast fading, which is then smoothed by explicit averaging, whereas the computation of the RTMV is much less expensive, because it requires field strength data only at a single point, and because the RTMV varies slowly with position, a much less dense grid of points can be used.

C. The Sabine Local Area Average

The Sabine method in acoustics [17] is based on the assumption that the volume-averaged energy density in a room is constant throughout the room. It has been extended to Electromagnetics in [18-21]. The Sabine method is applied in [18] to calculate the Q factor of a reverberation chamber, and the decay time, which depends on the volume, the angle-averaged power absorption coefficient of the surfaces, and on the surface area. The acoustical analogy is used in [19] to estimate the reverberation time and to calculate the power delay profiles in an indoor environment. For highly-absorbent or “dead” environments, [19] replaced the Sabine absorption by the Eyring formula. The formula for the reverberant field strength is given in [11] and the “reverberation distance” is defined as the distance from the source at which the direct field is equal to the reverberant field. In [18], power delay profiles based on the reverberation model are compared with measured power delay profiles, with good agreement. However, the Sabine method is not well known for calculating the coverage of an access-point antenna in a site specific model.

The Sabine method was extended in [22] so that it could be applied to estimate the field strength throughout a complex floor plan in a site-specific model. Then the Sabine method was used to assess the possibility of interference with medical devices due to a wireless local area network made up of several access point antennas and handheld terminals.

D. Objectives and Paper Organization

Ray tracing is widely used in site-specific studies to compute electric field strengths. Although it is difficult to obtain agreement between fast-fading electric field strengths computed with ray tracing and those obtained by measurement, it is generally accepted that the RTMV of equation (4) is a good predictor of the local mean value

computed by windowing measured data with equation (3). An objective of this paper is to assess the accuracy of the frequently-used RTMV against the RTLAA, that is, the local area average obtained by explicitly windowing closely-spaced field values. Similarly, an objective of this paper is to assess the accuracy of the Sabine local area average against the RTMV and the RTLAA.

First, this paper summarizes the Sabine method and extends it to be useful in long, narrow spaces such as a corridor, by introducing an exponential decay of the field strength with distance. Two problems have been selected to assess the accuracy of the computationally-fast RTMV and Sabine methods against the slower RTLAA and against measurements. The first is a room of rectangular shape, where the fast methods are expected to have good accuracy, and the second is a long, narrow corridor, where the fast methods are shown to be less accurate. In the rectangular room, it is shown that the RTLAA agrees reasonably with the measured field strength, and that both the RTMV and the Sabine field strength are reasonable approximations to the RTLAA. In the long corridor, the RTLAA field strength is similar in behaviour to the measured field strength. It is shown that, using the exponential decay term, the Sabine field strength in the corridor agrees reasonably with the RTMV. However, both fast methods underestimate the RTLAA field strength along the corridor centerline. Finally, when a small reflecting screen is placed behind the transmitter, it is shown that the Sabine method accounts poorly for the image of the source in the screen, and the field strength agrees poorly with the RTMV estimate. The two cases of the long corridor illustrate situations where the fast estimates should be used with caution.

II. THE SABINE METHOD

The Sabine method [17] is used in acoustics to determine the sound pressure level in a room or concert hall due to a source of acoustic power. It is assumed that the field of the source is reflected many times from the walls of the room, and that the energy density becomes uniform throughout the room at steady state, with the power radiated by the transmitter equal to the power absorbed by the room surfaces. It may be shown that the reverberant energy density is [21],

$$\tilde{\Psi}_{rev} = \frac{4P_r}{Ac} \quad \text{J/m}^3 \quad (5)$$

where P_r is the power radiated by the transmitter, c is the speed of light, and the room absorption is defined as,

$$A = \sum_{k=1}^N S_k \tilde{\alpha}_k \quad \text{m}^2 \quad (6)$$

where there are N different surfaces in the room, such as wall, doors, windows, floor, and ceiling, each of area S_k . The angle-averaged power absorption of a surface is [18],

$$\tilde{\alpha} = 2 \int_0^{\pi/2} \left[1 - \frac{1}{2} (|\Gamma_{\parallel}|^2 + |\Gamma_{\perp}|^2) \right] \sin \theta \cos \theta d\theta \quad (7)$$

where Γ_{\parallel} and Γ_{\perp} are the angle-dependent amplitude reflection coefficients for the parallel and perpendicular polarization, respectively. The angle-averaged power-absorption coefficient (7) for a slab wall model is readily evaluated by numerical integration of the reflection coefficients in [11]. Then given the floor plan of a room, the room absorption (6) can be found and used to find stored energy in the reverberant field with equation (5). The corresponding reverberant electric field strength \tilde{E}_{rev} is obtained by equating the energy density to that in a plane wave, $\tilde{\Psi}_{rev} = \epsilon \tilde{E}_{rev}^2$.

To calculate the field strength as a function of distance from the antenna, it is useful to split the field into the sum of the “direct” field, which is the field of the transmitter in free space, and the “multipath” or “indirect” field, which is sum of the fields associated with all the reflected and multiply-reflected rays that pass through the observer [22]. The energy density in the reverberant field, $\tilde{\Psi}_{rev} = \tilde{\Psi}_{dir} + \tilde{\Psi}_{in}$, is the sum of the energy density in the direct field $\tilde{\Psi}_{dir}$ and that in the indirect field, $\tilde{\Psi}_{in}$. If the walls of the room are perfectly absorbing, then there is no indirect field, $\tilde{\Psi}_{in} \rightarrow 0$, the wall absorption coefficients become unity, $\tilde{\alpha} = 1$, so the room absorption is equal to the total area of the walls, $A = S_T = \sum S_i$. As $A \rightarrow S_T$ and $\tilde{\Psi}_{in} \rightarrow 0$, the reverberant energy density $\tilde{\Psi}_{rev} \rightarrow \tilde{\Psi}_{dir}$. In equation (6), with perfectly-absorbing walls $A = S_T$ and $\tilde{\Psi}_{rev} = \tilde{\Psi}_{dir}$, so the energy density in the direct field is,

$$\tilde{\Psi}_{dir} = \frac{4P_r}{S_T c} \quad (8)$$

It follows that for a room of absorption A , the energy density in the indirect field is,

$$\tilde{\Psi}_{in} = \tilde{\Psi}_{rev} - \tilde{\Psi}_{dir} = \frac{4P}{A_{in} c} \quad (9)$$

where the indirect room absorption is,

$$A_{in} = \frac{AS_T}{S_T - A} \quad (10)$$

The corresponding electric field strength \tilde{E}_{in} obeys $\tilde{\Psi}_{in} = \epsilon \tilde{E}_{in}^2$, and so the indirect field strength is,

$$\tilde{E}_{in} = \sqrt{\frac{4\eta P_r}{A_{in}}} \quad (11)$$

where field strengths are given in V/m RMS. Note that if the walls are perfectly absorbing, then $A_{in} \rightarrow \infty$ and the indirect field becomes zero, as expected. Since the indirect field strength is based on the assumption of a uniform distribution of energy throughout the room, the tilde is used to indicate that \tilde{E}_{in} is a volume average.

The direct field strength of a wireless source radiating power P_t at distance r is given by,

$$E_{dir}(r) = \sqrt{\frac{\eta D P_t}{4\pi r^2}} \quad (12)$$

The directive gain of the source is D and η is the intrinsic impedance of free space. To estimate the mean value of the field strength, the direct and indirect fields are combined on an energy basis to obtain,

$$\tilde{E}_{Sab}(r) = \sqrt{\left(\frac{\eta D P_t}{4\pi r^2} \right) + \left(\frac{4\eta P_t}{A_{in}} \right)} \quad (13)$$

For distances very close to the transmitter, the direct field is much larger than the indirect field and equation (13) approaches the local field strength of the transmitter.

The Sabine method has been applied to realistic floor plans such as that in [22]. The room absorption of equation (10) is evaluated by a numerical approximation called the “patch method”. The walls, floor and the ceiling are subdivided into patches of area ΔS , of size approximately 25 cm square. The center of each patch is joined to the observer by a ray. If the ray is blocked by an intervening wall panel, then the patch is not line-of-sight to the observer, and does not contribute to the absorption. If the ray is not blocked, then the patch contributes $\tilde{\alpha} \Delta S$. The algorithm is very simple and fast in execution. The room absorption is then dependent on the location of the observer. If the observer is in a small room, the observer “sees” patches of wall that add up to a small total area, and lead to a small room absorption. But if the observer is in a large hall, the observer “sees” a large wall surface area and a large value for the room

absorption and the environment approaches free space behavior.

It will be demonstrated below that equation (13) provides a reasonable estimate in a box-shaped room, but that in a long corridor, equation (13) becomes increasingly in error with distance from the source. The following presents a novel correction factor for long corridors.

A. Correction for Long Narrow Spaces

Consider a long corridor of width w and height h . Let the power flowing through a cross-section wh of the corridor be $P(z)$, where z is distance from the transmitter along the corridor. For a slice of corridor of length dz , power $P(z)$ is the “source” for the reverberant field, and the energy density in the slice is given by equation (9) as $\tilde{\Psi}_{rev}(z) = 4P(z)/Ac$. From equation (6), the power incident on the surface area $2(w+h)dz$ of the slice is $(\tilde{\Psi}_{rev}c/4)(2(w+h)dz)$ and the decrease in power across the slice is,

$$dP = -\alpha \frac{\tilde{\Psi}_{rev}c}{4} (2(w+h)dz) \quad (14)$$

where $\alpha = A/S_T$ is the average power absorption coefficient for the surfaces, and A is the room absorption at the location of the slice. Thus the power obeys the first-order differential equation,

$$\frac{dP}{dz} + \frac{1}{\delta} P = 0 \quad (15)$$

where the “penetration depth” along the corridor is,

$$\delta = \frac{A}{2(w+h)\alpha} . \quad (16)$$

The power available to drive the reverberant field at distance z from the source is,

$$P(z) = P_t e^{-z/\delta} \quad (17)$$

where the power at $z=0$ is equal to the power transmitted by the source P_t . Exponential decay with distance is consistent with the attenuation of fields in waveguides.

A simple formula for the penetration depth was sought that could be applied to arbitrary observer locations in a complex floor plan. The ceiling height h is known and constant throughout the floor plan, but the width w is ambiguous, because it could be taken as either the length or the width of the room. To eliminate w it will be assumed that the “footprint” of the room has area w^2 .

With this assumption, the area of the walls, floor and ceiling is,

$$S_T = 2w^2 + 4wh . \quad (18)$$

In a complex floor plan, the room absorption A and the surface area S_T are found for any observer by the “patch method”. Then equation (18) is solved for w , and the penetration depth approximated as,

$$\delta = \frac{S_T}{\sqrt{4h^2 + S_T}} \quad (19)$$

where $\alpha = A/S_T$ has been used to eliminate the power absorption coefficient. With these assumptions, the penetration depth is a purely geometrical parameter, and is readily applied in the context of an observer embedded in a complex floor plan.

The indirect field is calculated with equation (11), where the power of the source P_t is replaced by the attenuated power of equation (19). The indirect field thus attenuates exponentially with distance from the source. It will be demonstrated below that this “corrected” indirect field is a good approximation of the ray-tracing mean value field strength in a long corridor.

III. APPLICATIONS

This section applies ray tracing and the Sabine method to calculate the field strength in a rectangular room and in a long, narrow corridor, and compares the results to measured field strengths.

A. The Rectangular Room

Measurements and simulations were done in a laboratory, shown in Fig. 1. The lab measured 6.83 m wide by 8.68 m deep, with a ceiling height of 3.75 m. The lab was rectangular in shape, and was quite different from the long, narrow corridor considered in the following section. It was filled with lab benches and equipment, which were not included in the simulation. The measurement setup was described in [23, 24]. The receive antenna was located on a phenolic tripod 1.61 m from a side wall and 4.97 m from the front wall of the room. The center of the receive antenna was 1.03 m above the floor. The receive antenna was an ETS Lindgren #3126 sleeve dipole, and the received power was measured by an HP8569B spectrum analyzer. The transmit antenna was carried by a moving platform or “robot” that followed tape stuck to the floor along a straight-line path starting 30 cm from the receiver and ending 4.92 m from the receiver. The transmitter consisted of a battery-operated oscillator at 2388 MHz driving a quarter-wave monopole

on top of a small aluminum box. The base of the monopole was 1.07 m above the floor. The system measured the received power every 1.5 cm along the path. Because the transmitted power was not known, the system was uncalibrated and the measured field strengths required scaling to match the transmitted power in the simulation.

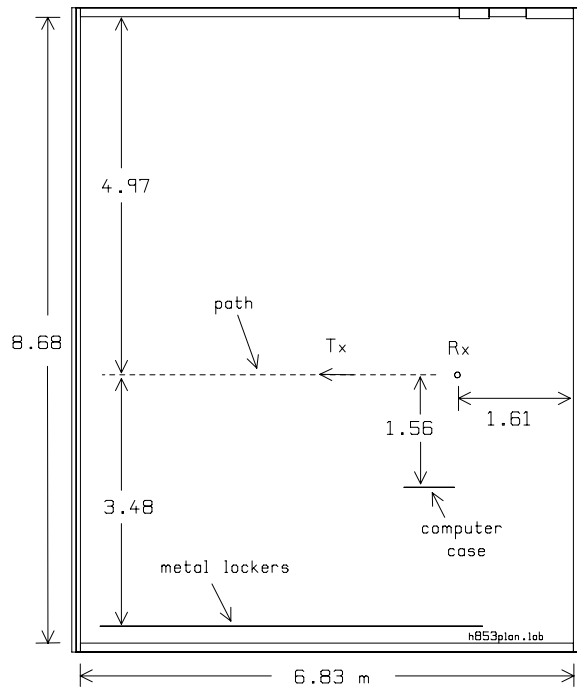


Fig. 1 Plan of the rectangular room.

The room of Fig. 1 was modelled for simulation by ray tracing. Each wall was modelled as a layered structure with 1.5 cm of concrete ($\epsilon_r=5.37$, $\sigma=149.5$ mS/m), 0.8 cm of brick ($\epsilon_r=4.38$, $\sigma=18.5$ mS/m), a center air layer 7.8 cm thick, and symmetric layers of brick and concrete. The floor and ceiling were modelled as concrete slabs of thickness 30 cm, with 3.75 m height from floor to ceiling. The room had various pipes and ducts below the ceiling, which were not included in the model. The near side of a metal computer case measuring 70 cm wide by 46 cm tall was 1.56 m from the path, and was included in the model because it was found to reflect the field very significantly. One wall of the room had a row of metal lockers, 3.48 m from the path, which were included in the model. But lab benches, other instruments, and other clutter in the room were not modelled. In the simulation, the transmitter was a vertical, half-wave dipole radiating 100 mW, with directivity $D=1.64$, and the transmitter was at the fixed location Rx in Fig. 1 while the receiver moved along the path. Ray paths with up to 32 reflections were calculated. Including more reflections did not change the result

substantially. The electric field strength was evaluated every 0.5 cm to trace the fast fading of the signal in detail, and then equation (4) was used to evaluate the RTLAA with a window size of 0.7 m.

Figure 2 compares the measurements and simulations in the rectangular room. The electric field strength in dB relative to 1 V/m is shown as a function of the separation between the transmitter and the receiver. The measured data was scaled such that the measured RMS value was equal to the RMS value of the simulated data in the distance interval 0.5 m to 2 m separation between the Tx and the Rx. To study the slow fading of the signal, the measured and simulated field strengths were “windowed” by taking the local area average over a 70 cm or 6-wavelength interval, using equation (2).

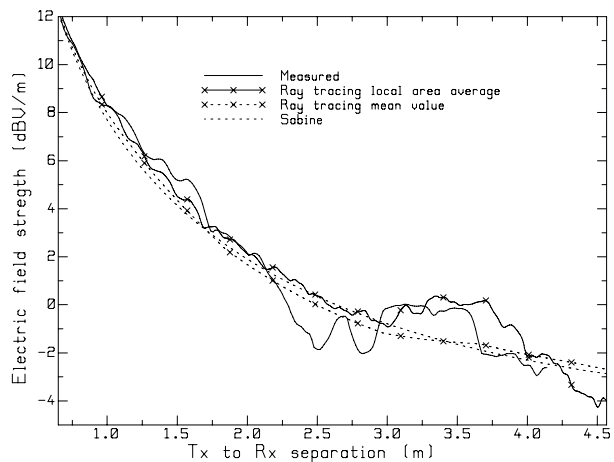


Fig. 2 Measurement and simulations in the rectangular room.

Figure 2 compares the scaled, measured field strength (solid line) with the RTLAA field strength (solid line with crosses) and shows reasonable agreement. At a separation of about 2.5 m, the measured field strength had a minimum not seen in the simulation, and the measured field was about 2.1 dB smaller than the simulation. At a separation of about 3.5 m, both the simulation and the measurement had a maximum. The RMS error between the measured curve (in dB) and the RTLAA curve (in dB) from 0.7 to 4.1 m separation was 0.90 dB, which we considered to be good agreement.

The RTMV field strength (not shown) of equation (5) had step discontinuities because rays switched in and out of the solution as the observer moved, for example due to reflections from the computer case. The RTMV was smoothed using equation (2) with a 70 cm window, and is shown in Fig. 2 by the dashed curve with crosses. For most of the path, the phasing of the rays was such that the RTMV estimate was smaller than the RTLAA by less than half a dB. The maximum at 3.5 m separation in the RTLAA is not seen in the RTMV estimate.

To evaluate the field strength using the Sabine method, the angle-averaged power absorption coefficient in equation (7) was found for the layered wall and for the concrete slab modelling the floor and ceiling. Then room absorption was found for each point along the path, using equation (6) evaluated by the patch method. For this simple rectangular-box room, the room absorption was about $A = 165$ square meters. The indirect absorption in equation (10) was about $A_m = 541$ square meters. For each point on the path, equation (12) was used to find the direct field and equation (11) was used to find the indirect field, and these were combined on an energy basis using equation (13) to find the Sabine estimate of the local mean field strength. The distance correction of equation (17) is intended for long, narrow spaces, and not rectangular rooms, and so was not used. For comparison with the windowed field strength from ray tracing, the Sabine field strength was averaged over a 70 cm window.

To compare the accuracy of the fast estimates of the local mean field strength with the much-more-computationally-expensive RTLAA value, Fig. 2 shows the RTMV field strength and the Sabine field strength, in comparison to the RTLAA estimate. The figure shows that the RTMV field strength (dashed curve with crosses) and Sabine field strength (dashed curve) were very close in value, with an RMS difference between them of 0.27 dB. The error between the RTMV and the RTLAA estimate was 0.82 dB; that between the Sabine field strength and the RTLAA estimate was 0.86 dB. Both of the quick estimates were within one dB of the much-more-computationally-costly RTLAA field strength. For the rectangular room, the Sabine method provided an accurate approximation of the behavior of the field with distance from the transmitter.

B. The Long Corridor

Figure 3 shows the plan of the 50.6 m corridor that was used to compare simulations with measurements. The rectangular room of the previous section is shown for comparison. The Sabine method assumes that the energy density is uniform throughout the volume of the space, which was a reasonable assumption for the rectangular room, but not for the corridor, where the length was much longer than the width. The distance correction in equation (17) models the energy density as declining exponentially along the corridor and it will be shown that this was in reasonable agreement with the RTMV estimate.

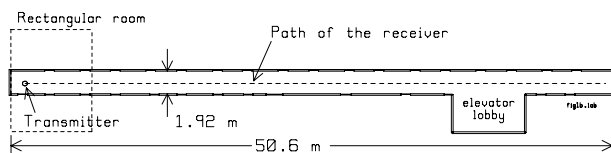


Fig. 3 The geometry of the 50.6 m corridor.

The corridor of Fig. 3 was 50.6 m long and 1.92 m wide. The corridor had a hanging ceiling at 2.27 m height. Above the hanging ceiling, there was wiring, pipes and ducting which were not included in the simulation model. The bottom of the concrete slab for the next floor of the building was at a height of 2.75 m. The transmit antenna for the simulations and the measurements was 1.6 m above the floor and 1.2 m from the end wall, and was in the center of the corridor, 0.96 m from each side wall. The receiver was moved along a path at height 1.6 m above the floor along the centerline of the corridor for a distance of about 50 m. Measurements and simulations were done at 850 MHz.

The end wall behind the transmitter was of glass-block construction of thickness about 10.2 cm. There was a window inserted into the glass-block wall, measuring 63 cm wide and 43 cm tall. Two different corridors were measured. For the eighth floor corridor, there was no insect screen in the window, but for the fifth floor corridor the window had a metal insect screen. The transmitter was approximately centered on the metal window screen on the fifth floor, and the screen reflected the field effectively, and profoundly changed the field strength in the corridor. It will be demonstrated below that the Sabine method accounts poorly for the window screen.

The measurements were done using the system described in [25]. The transmitter was a Motorola SLF1690C analog cellular telephone, programmed to transmit continuously at its full power of 600 mW, and the power transmitted was monitored periodically. The base of the cell phone's antenna was 1.6 m above the floor and approximately 1.2 m from the glass-block end wall, and 0.96 m from the side walls. The receive antenna was an Electromechanics 3121C-dB4 dipole, of length one-half wavelength at 850 MHz or 17.65 cm, oriented vertically. The receive antenna was carried by a moving platform or "robot" along the corridor centerline, and was supported on a stand made of PVC pipes with the dipole's midpoint 1.6 m above the floor. The received power was measured with an Anritsu MS2610B spectrum analyzer. The receive dipole was connected to the spectrum analyzer by a cable of length approximately 10 m. As the robot moved, the received power was recorded at 30 cm (0.85 wavelength) intervals. The measurement points were too far apart to trace the fast fading of the field strength.

For the ray-tracing simulation, the transmit antenna was represented as a vertical half-wave dipole antenna radiating 600 mW at 850 MHz, and so the field incident on the side walls and end walls of the corridor had the "perpendicular" polarization. The walls of the corridor were of clay block construction and were modelled for simulation with five layers: plaster ($\epsilon_r = 6.1$, $\sigma = 60.1$ mS/m) of thickness 1.5 cm; brick ($\epsilon_r = 5.1$, $\sigma = 10$ mS/m)

of thickness 0.8 cm; and air space 9.2 cm thick; and symmetrical layers of brick and plaster. The reflection coefficient for the perpendicular polarization was about 0.8 for 0 degree or “normal” incidence; 0.86 at 70 degrees from the normal; and rising to unity for grazing incidence. The concrete slab floor and ceiling were 30 cm thick and were represented with $\epsilon_r=6.1$ and $\sigma=60.1$ mS/m. The doorways were filled with wood doors ($\epsilon_r=2.5$, $\sigma=1.18$ mS/m) 10 cm thick, except for the fire door near the antenna, which was metal. The glass block end walls were modelled with a 0.5 cm layer of glass ($\epsilon_r=4$), a 9.6 cm air layer, and a symmetric 0.5 cm glass layer. The reflection coefficient for the perpendicular polarization was less than 0.1 for incidence from the normal to about 50 degrees from the normal, and then rose rapidly to unity for grazing incidence. Thus, the glass block end wall was almost transparent over a wide range of angles of incidence. On the eighth floor, the window in the glass-block wall had no metal screen. But on the fifth floor, the window had a metal insect screen which was modelled as perfectly reflecting.

In ray-tracing simulations, computational error can be reduced by increasing the number of reflections. Sufficient reflections have been accounted for when little change is seen by including further reflections. For this study, the field strength along the corridor centerline was examined as the number of reflections was increased. The field strength with three reflections agreed reasonably with that using 14 reflections to a distance of about 15 m along the hallway. Five reflections were sufficient to about 20 m distance; seven to 30 m distance; ten reflections to about 40 m. The broad minimum in the local field strength around 42.5 m distance and the maximum around 46 m distance required 14 reflections to be tracked. Computing more than 14 reflections did not substantially change the field in the corridor, and so 14 reflections were used in the results that follow.

Eighth Floor: Figure 4 shows measured and simulated field strength along the corridor on the eighth floor. Ray tracing was used to compute the field strength at 1 cm intervals and the RTLAA was calculated with equation (3) using a 2 m window size, which is 5.7 wavelengths at 850 MHz. To scale the measured values to the same radiated power as the simulations, the RMS value from 1.6 m to 3 m separation between the Tx and the Rx was made equal to the RMS value of the RTLAA field strength. The measured data was also averaged with a 2 m window, which used six measured points at 30 cm separation.

Figure 4 compares the measured field strength (solid curve) with the RTLAA field strength (solid curve with crosses). Both the measured and simulated field strengths had a broad maximum at 9.5 m distance, and again at 22 m distance and 36 m distance. The measured field

strength was larger than the RTLAA field strength from 11 m to 16 m distance. The measured field had a peak at 29 m distance whereas the simulation had a minimum. The general behaviour of the measured and simulated field strength was similar although details differed. In the separation interval from 1.6 m to 44.5 m, the RMS error between the measured field strength and the RTLAA field strength was 2.17 dB.

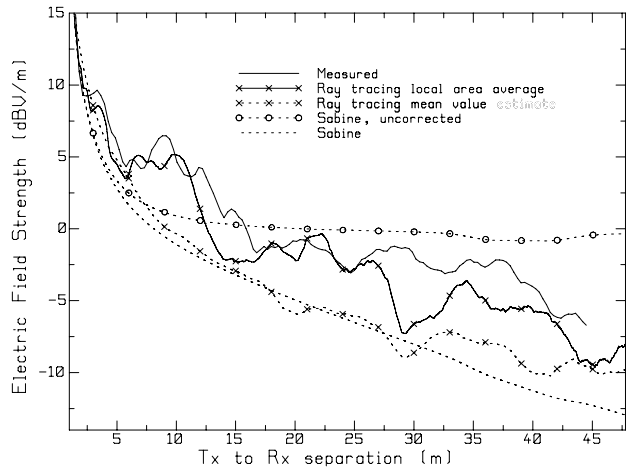


Fig. 4 Measurement and simulations on the eighth floor corridor.

The dashed curve with crosses in Fig. 4 shows the RTMV estimate in equation (4) after smoothing with a 2 m window. It might be expected that the RTMV curve would pass through the “average” of the RTLAA curve. Yet in Fig. 4, the RTMV estimate was less than the RTLAA field strength for separations greater than about 6 m. The RTMV combines the ray amplitudes on an energy basis to obtain an estimate of the mean value, which assumes that the fields have random phase angles with a uniform distribution. But with the transmitter and receiver on the centerline of the corridor, the path lengths for reflections from the left wall and right wall were identical, and rays arrived in phase, violating the assumption of random phase. This problem is one where the RTMV is not a good estimate of the true local area average field strength. The RMS error between the RTMV and the RTLAA values was 3.13 dB.

The Sabine model of the corridor had absorption of about $A=314$ square meters, about twice that of the rectangular room. The indirect absorption was about $A_m=968$ square meters, again about twice the value for the rectangular room. The dashed curve with circles shows the Sabine estimate given by equation (13). For “close” separations less than about 6 m, the Sabine field strength was about 2 dB less than the RTMV estimate. For separations greater than about 10 m, the Sabine field strength in Fig. 4 was much too large. For distances where the direct field strength is much less than the

indirect field strength, equation (13) predicts that the net field strength should be approximately constant and equal to the indirect field. Thus, towards the end of the corridor, the Sabine approximation became approximately constant and was not a good approximation to the ray-tracing mean value field strength. The distance correction of equation (17) introduces an exponential reduction in the indirect field with distance along the corridor and the field strength is shown by the dashed curve in Fig. 4, and was a reasonable approximation of the RTMV field strength. The RMS error between the Sabine field strength including the distance correction and the RTLAA field strength was 3.93 dB. The Sabine field strength and the RTMV field strength were in reasonable agreement, with an RMS error of 1.36 dB between them,

Figure 4 shows that neither the RTMV nor the Sabine field strength is a good approximation of the RTLAA field strength along the centerline of a long corridor. Thus the fast methods should be used with caution in this situation.

Fifth Floor: The wall construction of the eighth and fifth floors appeared to be very similar and it would be expected that the slow fading of the field strengths would be similar. However, the measured curves for the fifth floor (Fig. 5) and eighth floor (Fig. 4) were quite different. This difference arose partly because there was a metal screen in the window directly behind the transmitter on the fifth floor, separated from the antenna by 121 cm. The metal screen strongly reflected the field so that the antenna and its image in the metal screen behaved as a two-element array, with the antenna and its image separated by about 6.88 wavelengths. For an observer in the far field of the array in the direction of the corridor centerline, the phasing of the field of the transmitter and of its image in the screen was such that the net field strength was 1.14 dB less than that of the transmitter alone. On the eighth floor, the glass-block wall was almost transparent and contributed little to the field in the corridor. But on the fifth floor, the metal screen reflected substantially into the corridor. An observer on the corridor centerline would see two sets of rays. One set would be the same as the rays seen in the eighth floor corridor. The second set would be rays that reflected from the screen behind the transmitter and then found their way to the observer. Thus, the mean value of the multipath field would be approximately doubled. The RTMV estimate of equation (4) was larger on the fifth floor than on the eighth floor because about twice as many rays passed through the observer.

Figure 5 shows the measured field, smoothed with a 2 m window (solid curve) and the RTLAA simulated field strength (solid curve with crosses). The large maximum at 8.5 m separation was seen in both the measurement and the simulation. The rapid decline in the measured field from 10 m to 13 m separation was

reproduced well in the simulation. There was a maximum in the measured field at 17.5 m distance, and a corresponding but larger maximum in the simulated field strength. For larger distances the measurement and simulation did not align as well.

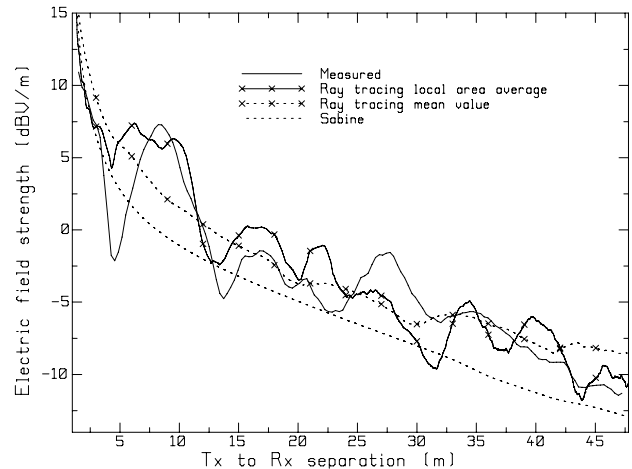


Fig. 5 Measurement and simulations on the fifth floor corridor.

The sharp minimum at 4.5 m distance in the measured field strength was not reproduced in the simulation. If the wall model were changed to have three layers, $\epsilon_r=3$ for 2.3 cm thickness on both surfaces, separated by a 9.4 cm air layer, then the reflection coefficient for the perpendicular polarization at 69 degrees incidence from the normal would be zero, and the wall would not reflect fields from the transmitter to the receiver for separations around 5 m. Then the simulated field strength would have a sharp minimum like that in the measurement. However, the walls on the eighth floor and the fifth floor appeared to have similar construction, and it did not seem reasonable to use a different wall model in the simulations for the eighth and fifth floors.

The RMS error between the RTLAA field strength and the measured field strength in the distance interval from 1.6 m to 44.5 m was 2.37 dB, not quite as good agreement as the error of 2.17 dB found for the eighth floor.

The ray-tracing approximation accounted quite well for the metal screen in the window behind the transmitter, by calculating ray paths that reflect from the screen. The RTMV field strength estimate with the screen in Fig. 5 was larger than that with no screen in Fig. 4, and was a reasonable approximation of the much-more-expensive RTLAA estimate. The RMS error between the RTMV field strength and the RTLAA field strength was 1.9 dB.

The fifth floor results illustrate a situation where the Sabine method performed poorly. The Sabine calculation did not explicitly evaluate reflection paths and so could not account directly for the image of the transmitter in the

screen. Instead, the presence of the screen was accounted for by its angle-averaged power absorption coefficient of zero, replacing the power absorption of window opening with no screen, which was unity. But the surface area of the 63 cm \times 43 cm screen was very small compared to the surface area of the entire hallway, and so the change in the room absorption of equation (6) was negligible. Hence the indirect field hardly changed at all due to the presence of the screen. The Sabine estimate of the field strength for the fifth floor was the same as that for the eighth floor, and agreed poorly with the RTLAA estimate, with an error of 3.4 dB, not nearly as good as the agreement of the RTMV estimate. Thus, when a transmitter is close to a highly-reflecting surface, the Sabine method should be used with caution.

IV. CONCLUSION

This paper has compared computationally-fast estimates of the local-area-average field strength with the much-slower detailed ray-tracing calculation, and with measurements. The “fast” estimates are firstly, the ray-tracing mean value given by equation (4), which is a slowly-varying function and can be computed at widely separated points, and secondly, the Sabine method given by equation (13), which is obtained by a very simple calculation. Conversely, a detailed ray-tracing calculation uses a dense grid of points to calculate the fast fading of the field, and then explicitly averages the field with equation (3), to obtain the RTLAA estimate, and is therefore a computationally-expensive calculation.

In a typical rectangular room, the agreement of the RTLAA field strength with the measurement was good. Both the RTMV estimate and the Sabine estimate were good approximations to the RTLAA field strength.

The long corridor problem illustrated that the fast methods can have significant errors. The RTLAA estimate of the field strength along the centerline of the corridor was generally larger in value than the RTMV estimate, with an RMS error of about 3.1 dB. The Sabine estimate was poor for the long corridor unless the exponential distance correction of equation (17) was used. With the distance correction, the Sabine estimate differed from the RTMV estimate by 1.4 dB and from the RTLAA estimate by 3.9 dB.

The fifth floor corridor illustrated that the Sabine method was inaccurate when a small reflecting screen was located behind the transmitter. Ray tracing accounted well for rays reflected from the screen, and the RTMV field strength was about 2 dB different from the RTLAA value. But the Sabine method accounted for the screen only through the change in the room absorption, which was negligible because the area of the screen was small compared to the overall surface area of the corridor. The error in the Sabine method was 3.4 dB, much poorer than the error in the RTMV estimate.

This paper has shown that the RTLAA field strength agrees reasonably with measurements for both the rectangular room and the long corridor. The significance of this paper is that it establishes that both the commonly-used RTMV estimate and the little-known Sabine field strength estimate are accurate in a rectangular room, but are less accurate in a long, narrow corridor. The Sabine method provides a computationally-inexpensive estimate of the field strength in rectangular rooms, and can be readily extended to complex floor plans with multiple sources.

ACKNOWLEDGEMENT

The authors gratefully acknowledge the support of PROMPT, Bell Canada, Nortel, FQRNT, and National Science and Engineering Research Council of Canada.

REFERENCES

- [1] H. Hashemi, “The indoor propagation channel,” *Proc. IEEE*, vol. 81, no. 7, pp. 943-968, July 1993.
- [2] J. B. Andersen, T. S. Rappaport, and S. Yoshida, “Propagation measurement and models for wireless communication channels,” *IEEE Communications Magazine*, vol. 33, no. 1, pp. 42 – 49, Jan. 1995.
- [3] C.-P. Lim, J. L. Volakis, K. Sertel, R. W. Kindt, and A. Anastasopoulos, “Indoor propagation models based on rigorous methods for site-specific multipath environments,” *IEEE Trans. on Ant. and Prop.*, vol. 54, no. 6, pp. 1718-1725, June, 2006.
- [4] J. M. Gorce, K. Jaffres-Runser, and G. de la Roche, “Deterministic approach for fast simulations of indoor radio wave propagation,” *IEEE Trans. on Ant. and Prop.*, vol. 55, no. 3, pp. 938-948, March 2007.
- [5] Z. Yun, M. F. Iskander, and Z. Zhang, “Complex-wall effect on propagation characteristics and MIMO capacities for an indoor wireless communication environment,” *IEEE Trans. on Ant. and Prop.*, vol. 42, no. 4, pp. 914- 922, April 2004.
- [6] H. Bertoni, W. Honcharenko, L. R. Maciel, and H. H. Xia, “UHF propagation prediction for wireless personal communications,” *Proc. IEEE*, vol. 82, no. 9, pp. 1333-1359, Sept. 1994.
- [7] T. S. Rappaport, *Wireless Communications, Principles and Practice*. New Jersey: Prentice-Hall PTR, 1996.
- [8] K. W. Cheung, J. H. M. Sau, and R. D. Murch, “A new empirical model for indoor propagation prediction,” *IEEE Trans. on Veh. Tech.*, vol. 47, no. 3, pp. 996-1001, Aug. 1998.
- [9] V. Degli-Esposito, G. Lombardi, C. Passerini, and G. Riva, “Wide-band measurement and ray-tracing simulation of the 1900 MHz indoor propagation channel: comparison criteria and results,” *IEEE*

- Trans. on Ant. and Prop.*, vol. 49, no. 7, pp. 1101-1110, July 2001.
- [10] D. Didascalou, J. Maurer, and W. Wiesbeck, "Subway tunnel guided electromagnetic wave propagation at mobile communication frequencies," *IEEE Trans. on Ant. and Prop.*, vol. 49, no. 11, pp. 1590-1596, Nov. 2001.
- [11] E. H. Newman, *Plane Multilayer Reflection Code*. Technical Report 712978-1, ElectroScience Laboratory, The Ohio State University, July 1980.
- [12] R. A. Valenzuela, O. Landron, and D. L. Jacobs, "Estimating local mean signal strength of indoor multipath propagation," *IEEE Trans. on Veh. Tech.*, vol. 46, no. 1, pp. 203-212, Feb. 1997.
- [13] F. Van Der Wijk, A. Kegel, and R. Prasad, "Assessment of a pico-cellular system using propagation measurements at 1.9 GHz for indoor wireless communications," *IEEE Trans. on Veh. Tech.*, vol. 44, no. 1, pp. 155-162, Feb. 1995.
- [14] R. Tingly and K. Pahlavan, "Space-time measurement of indoor radio propagation," *IEEE Trans. on Inst. and Meas.*, vol. 50, no. 1, pp. 22-31, Feb. 2001.
- [15] T. M. Schafer, J. Maurer, J. Von Hagen, and W. Wiesbek, "Experimental characterization of radio wave propagation in hospitals," *IEEE Transactions on EMC*, vol. 47, no. 2, pp. 304-311, May 2005.
- [16] D. Lee, M. J. Neve, and K. W. Sowerby, "The impact of structural shielding on the performance of wireless systems in a single floor office building," *IEEE Trans. on Wireless Comm.*, vol. 6, no. 5, pp. 1787-1795, May 2007.
- [17] L. E. Kinsler, A. R. Frey, A. B. Coppens, and J. V. Sanders, *Fundamentals of Acoustics*, New York: Wiley, 2000.
- [18] D. A. Hill, "A reflection coefficient derivation for the Q of a reverberation chamber," *IEEE Trans. on EMC*, vol. 38, no. 4, pp. 591-592, Nov. 1992.
- [19] C. L. Holloway, M. G. Cotton, and P. McKenna, "A model for predicting the power delay profile characteristics in a room," *IEEE Trans. on Veh. Tech.*, vol. 48, no. 4, pp. 1110-1120, July 1999.
- [20] C. L. Holloway, D. A. Hill, J. M. Ladbury, and G. Koepke, "Requirements for an effective reverberation chamber: loaded or unloaded," *IEEE Trans. on EMC*, vol. 48, no. 1, pp. 187-194, Feb. 2006.
- [21] J. B. Andersen, J. O. Nielsen, G. F. Pedersen, G. Bauch, and M. Herdin, "Room electromagnetics," *IEEE Ant. and Prop. Mag.* vol. 49, no. 2, pp. 27-33, April 2007.
- [22] C. W. Trueman, S. S. Muhlen, D. Davis, and B. Segal, "Field strength estimation in indoor propagation by the Sabine method," in *Proceedings of the 24th Annual Review of Progress in Applied Computational Electromagnetics*. Niagara Falls, Ontario, Canada: ACES, pp. 876-881, 2008.
- [23] W. Muneer, I. Abdallah, D. Davis, and C. W. Trueman, "A novel automated site survey system," in *Proceedings of the Symposium on Antenna Technology and Applied Electromagnetics*. Montreal, Quebec, Canada: ANTEM, pp. 147-150, 2006.
- [24] W. Muneer, *Rician-K Factor Study for Temporal and Spatial Variations*, M.A.Sc. Thesis, Dept. of Electrical and Computer Engineering, Concordia University, Dec. 2007.
- [25] D. Davis, *Indoor Radio-Wave Behavior at 850 and 1900 MHz with Electromagnetic Compatibility Applications in Hospitals: An Experimental, Theoretical, Statistical and Morphological Characterization*, PhD. Dissertation, Dept. of Electrical and Computer Engineering, McGill University, Montreal, Quebec, Canada, 2003.



Christopher W. Trueman received his Ph.D. from McGill University in 1979. He has applied the methods of computational electromagnetics to problems such as aircraft antenna performance, antenna-to-antenna coupling and EMC on aircraft, aircraft and ship radar cross-section at HF frequencies, suppression of scattering of the signal of a commercial radio station from power lines, dielectric resonators, unconditionally-stable formulations for the finite-difference time-domain method, and the fields of portable radios such as cellular phones held against the head. Recently, his research has investigated the radar cross-section of ships at VHF frequencies, composite materials for aircraft, indoor propagation, and EMC issues between portable radios and medical equipment. Dr. Trueman is currently the Chair of the Department of Electrical and Computer Engineering at Concordia University.



Bernard Segal is a highly-interdisciplinary Research Engineer (Electrical Engineering, with a Master's in Electrical (Biomedical) Engineering and a PhD in Neurophysiology, all from McGill University). He is an Associate Professor in the Ear-Nose-Throat (ENT) Department of McGill University, with appointments in Biomedical Engineering and in Physiology. He is the Director of Research in ENT at McGill, and at the SMBD-Jewish General Hospital. He is the Director of Graduate Studies in ENT at McGill. He has contributed to many medical-EMC standards, EMC-healthcare policies, and EMC-healthcare recommendations. He has organized over thirty national

and international conferences, workshops and teaching sessions on EMC in Healthcare. His current research is directed towards clarifying the nature of electromagnetic-interference risk in hospitals, towards minimising this risk, and towards evaluating how to best use wireless informatics in health care safely.



Donald P. Davis received the B.Eng in electrical engineering degree from Concordia University in 1991, the MaSc. degree in electrical engineering from Concordia University in 1994 and the PhD. Degree in electrical engineering from McGill University 2004. Since 1995 he has been a sessional instructor teaching both graduate and undergraduate engineering courses at Concordia University. In 2006 he joined the Jewish General Hospital of Montreal as a post-doctoral researcher studying electromagnetic compatibility of medical equipment due to the presence of wireless communication systems. His research interests include indoor radio wave propagation measurement and modeling, electromagnetic interference estimation and safe implementation of wireless communication systems within clinical environments.



Wadah M. Muneer received his M.A.Sc. degree from Concordia University in 2007 under the supervision of Dr. Trueman. His research was in the field of indoor propagation for wireless channels. Wadah built an indoor automated site-survey system. This system was used in his research for taking measurements in two environments, a hallway and a microwave lab. The results obtained were used to estimate the Rician-K factor using four methods from literature, and compare them with K factor values obtained from simulating the two measurement environments using geometrical optics. Wadah is now a PhD student in the Department of Electrical and Computer Engineering at the University of British Columbia.